Journal of Biomedical Optics

SPIEDigitalLibrary.org/jbo

Probing the fractal pattern and organization of *Bacillus thuringiensis* bacteria colonies growing under different conditions using quantitative spectral light scattering polarimetry

Paromita Banerjee
Jalpa Soni
Harsh Purwar
Nirmalya Ghosh
Tapas K. Sengupta

SPIE

Probing the fractal pattern and organization of *Bacillus thuringiensis* bacteria colonies growing under different conditions using quantitative spectral light scattering polarimetry

Paromita Banerjee,[a*] Jalpa Soni,[b*] Harsh Purwar,[b] Nirmalya Ghosh,[b] and Tapas K. Sengupta[a]
[a]Indian Institute of Science Education and Research Kolkata, Department of Biological Sciences, Mohanpur Campus, P. O. Bidhan Chandra Krishi Viswavidyalaya, Kolkata, West Bengal 741252, India
[b]Indian Institute of Science Education and Research Kolkata, Department of Physical Sciences, Mohanpur Campus, P. O. Bidhan Chandra Krishi Viswavidyalaya, Kolkata, West Bengal 741252, India

Abstract. Development of methods for quantification of cellular association and patterns in growing bacterial colony is of considerable current interest, not only to help understand multicellular behavior of a bacterial species but also to facilitate detection and identification of a bacterial species in a given space and under a given set of condition(s). We have explored quantitative spectral light scattering polarimetry for probing the morphological and structural changes taking place during colony formations of growing *Bacillus thuringiensis* bacteria under different conditions (in normal nutrient agar representing favorable growth environment, in the presence of 1% glucose as an additional nutrient, and 3 mM sodium arsenate as toxic material). The method is based on the measurement of spectral 3×3 Mueller matrices (which involves linear polarization measurements alone) and its subsequent analysis via polar decomposition to extract the intrinsic polarization parameters. Moreover, the fractal micro-optical parameter, namely, the Hurst exponent H, is determined via fractal-Born approximation-based inverse analysis of the polarization-preserving component of the light scattering spectra. Interesting differences are noted in the derived values for the H parameter and the intrinsic polarization parameters (linear diattenuation d, linear retardance δ, and linear depolarization Δ coefficients) of the growing bacterial colonies under different conditions. The bacterial colony growing in presence of 1% glucose exhibit the strongest fractality (lowest value of H), whereas that growing in presence of 3 mM sodium arsenate showed the weakest fractality. Moreover, the values for δ and d parameters are found to be considerably higher for the colony growing in presence of glucose, indicating more structured growth pattern. These findings are corroborated further with optical microscopic studies conducted on the same samples. [DOI: 10.1117/1.JBO.18.3.035003]

Keywords: optical polarization; turbid medium polarimetry; Mueller matrix; light scattering spectroscopy; biological and medical applications; fractals; multiple scattering; *Bacillus thuringiensis*.

Paper 12664R received Oct. 6, 2012; revised manuscript received Jan. 19, 2013; accepted for publication Feb. 11, 2013; published online Mar. 5, 2013.

1 Introduction

Bacteria, as living organisms, are unicellular in nature, but in order to cope with environmental conditions, particularly under an unfavorable one, bacterial cells of the same species have evolved with time to develop cooperative behavior among them for survival.[1–3] This cooperative behavior have caused further evolving complex growth patterns in a bacterial colony.[4,5] Although a major part of the nature of colony growth and pattern formation depends on the type or species of bacteria as cellular machineries, bacteria also undergo major changes in response to environmental conditions such as availability of nutrients, temperature, thickness and hardness of the supportive surface, and presence of toxic materials.[4,6] Thus a growing colony of bacteria move along different directions to hunt food for their physiological growth and reproduction. In order to do these, bacterial cells in a growing colony cooperate through interactions to cope with the surrounding environmental conditions that result in a distinct and specific pattern formation as its signature, which in turn helps detection and identification of a bacterial species in a given space and under a given set of conditions.[7,8]

Extensive studies have been conducted to understand structural and molecular properties, and physiochemical regulations of bacterial colony growth and pattern formation.[9–13] Beneficial effects of multicellular growth and pattern formation by bacterial species in providing defense and/or survival mechanisms against adverse environmental conditions are well documented in the literature.[11–13] On the other hand, specific bacterial associations and colony growth patterns under different conditions have enabled us to identify and detect specific bacterial species and also helped us to understand cellular and molecular basis of signaling network for bacterial competition and cooperation.[3,12,13] Development of methods for quantification of cellular association and fractal (self-similar) patterns in

*These authors contributed equally to this work.

Address all correspondence to: Nirmalya Ghosh, Indian Institute of Science Education and Research Kolkata, Department of Physical Sciences, Mohanpur Campus, P. O. Bidhan Chandra Krishi Viswavidyalaya, Kolkata, West Bengal 741252, India. Tel: 91-9734678247; Fax: 91 33 2587 3020; E-mail: nghosh@iiserkol.ac.in; or Tapas K. Sengupta, Indian Institute of Science Education and Research Kolkata, Department of Biological Sciences, Mohanpur Campus, P. O. Bidhan Chandra Krishi Viswavidyalaya, Kolkata, West Bengal 741252, India. Tel: 91-9831417327; Fax: 91 33 2587 3020; E-mail: senguptk@iiserkol.ac.in

growing bacterial colony is therefore of considerable current interest.[14–18]

Elastic light scattering measurements is one such promising approach that can be exploited to gather quantitative morphological information on bacterial colony growth.[16–18] This follows because elastically scattered light from biological samples contain a wealth of morphological information, which if accurately extracted/quantified can serve as potential metrics for characterization of biological samples (including bacterial colony). Note that quantitative information on sample morphology can be obtained by either analyzing the angular variation or the wavelength variation of the elastic scattering signal.[19–21] This would, however, involve appropriate modeling of light scattering in complex biological systems and development of suitable inverse analysis methods to extract/quantify the morphological information contained in the elastic scattering signal.[19–21] In case of bacterial colony growth, the fractal nature of the colony is expected to have its characteristics impact the elastic scattering signal, via the corresponding self-similarity in the microscale fluctuations of local refractive index.[22–26] Indeed, several studies have explored development of inverse light scattering models based on fractal-Mie or fractal-Born approximation of light scattering, for the quantification of the self-similarity of refractive index fluctuations in biological samples.[22–26] These studies have revealed an inverse power law dependence of either the spectral or the angular variation of elastic scattering signal from such fractal biological structures, and the corresponding self-affinity has also been successfully quantified via the fractal micro-optical parameters (namely, the Hurst exponent, H, or fractal dimension, D_f) derived using fractal-Born approximation.[22–25] Such inverse light scattering based approaches are thus expected to provide quantitative information on the fractal growth of bacterial colony under different conditions. Since polarization properties of light scattered from samples contain additional microstructural and functional information on local organization, orientation of the scattering objects (which are otherwise hidden in polarization-blind optical measurements) and the combination of polarimetry with light scattering spectroscopy may yield complementary and useful information on the structural changes in the growth pattern of bacterial colonies. Specifically, the intrinsic sample polarization parameters, namely, the diattenuation, retardance, and depolarization coefficients[27–29] and their wavelength variation may be exploited in combination with the fractal micro-optical properties, for quantitative assessment of the bacterial colony growth. However, extraction/quantification and unique interpretation of these intrinsic polarimetry characteristics in complex biological systems are severely confound by (1) simultaneous occurrences of several polarization effects and (2) by multiple scattering effects.[27,28] The former effect causes lumping of several intrinsic polarimetry characteristics into the measurable polarization signal, leading to difficulties in their analysis and unique interpretation. While the latter effect, multiple scattering, not only causes extensive depolarization but also alters the polarization state of the residual polarization-preserving signal in a complex fashion.[27,28] Note that both of these confounding effects are expected to be present in the bacterial colony samples. Recent studies have demonstrated that measurement of Mueller matrix (a matrix that describes the transfer function of any medium in its interaction with polarized light[29,30]) and its inverse analysis via polar decomposition can be explored to tackle these problems.[31–33] The efficacy of such Mueller matrix decomposition approaches to delineate individual intrinsic polarimetry characteristics have also been validated in complex scattering media such as biological systems.[34–37] In this paper, we have thus employed such a generalized method for polarimetry analysis in combination with light scattering spectroscopy (and fractal-Born approximation-based inverse light scattering model), for simultaneous extraction/quantification of the intrinsic polarimetry characteristics and the fractal micro-optical parameters of growing bacterial colonies to probe the structural changes taking place during the colony formations under different conditions.

In our previous study, we have shown that for agriculturally and medically important bacteria *Bacillus thuringiensis*, higher concentrations of glucose cause catabolic repression of flagella expression and affects swarming motility of this bacterium on semi-solid nutrient agar plates.[8] Microscopic observations and theoretical modeling, based on reaction-diffusion, revealed how growing colonies of *Bacillus thuringiensis* cooperate in the form of bacterial association in presence of high glucose concentration and exhibit glucose-induced fractal pattern formation on agar plates.[8] As previously mentioned, since the pattern of a growing bacterial colony depends critically on the organization of the bacteria while they are in search for food, combined polarimetry and inverse light scattering spectroscopic analysis from the periphery of such growing colony can offer a potentially useful probe to look at the association between bacteria during growth, and hence can lead to the understanding of their behavior. In the present study, we have thus explored such possibility by conducting spectral Mueller matrix measurements on *Bacillus thuringiensis* colonies, grown on agar plates under three different conditions (in normal nutrient agar representing favorable growth environment, in presence of 1% glucose as additional nutrient but under catabolic repression for flagella mediated swarming motility, and 3 mM sodium arsenate as toxic material). Instead of the conventional 4×4 Mueller matrix, we have recorded a subset, the 3×3 Mueller matrix and its spectral dependence.[37] The use of the 3×3 Mueller matrix is motivated by the fact that it requires measurements using linear polarization alone and is thus particularly suitable for spectroscopic measurements (measurement at multiple wavelengths).[37] The wavelength variation of the elements of the measured 3×3 Mueller matrix were then subjected to the polar decomposition analysis to yield the intrinsic polarization parameters, namely, the linear diattenuation [$d(\lambda)$], linear retardance [$\delta(\lambda)$], and linear depolarization [$\Delta(\lambda)$] coefficients. The same decomposition analysis was also utilized to extract the spectral dependence of the polarization-preserving component of the scattered light, which was subsequently analyzed using the inverse light scattering model based on fractal-Born approximation,[22] to yield the Hurst exponent, H, of the *Bacillus thuringiensis* colonies under different growth conditions. The findings of the polarimetry and light scattering spectroscopic measurements/analysis were corroborated further with optical and electron microscopic studies conducted on the same samples. The results of these investigations are reported in this paper.

The paper is organized as follows. In Sec. 2, we provide a brief account of the 3×3 Mueller matrix decomposition. This is followed by a description of light scattering inverse analysis strategy for the estimation of fractal properties. Section 3 describes our experimental system for 3×3 spectral Mueller matrix measurement. The results of the spectral light scattering

polarimetric measurements on the bacterial colony samples are presented and discussed in Sec. 4. This include results of both the fractal parameters and intrinsic polarimetry characteristics, estimated from spectral light scattering inverse analysis and polar decomposition of Mueller matrix, respectively. The paper concludes with a discussion on the prospects of quantitative spectral light scattering polarimetry for *in situ* monitoring, detection, and identification of a bacterial species.

2 Theory

The Mueller matrix (a 4×4 matrix) represents the transfer function of an optical system in its interactions with polarized light and contains complete information about all the medium polarization properties in its various elements.[27–30] However, as mentioned previously, when several polarization events occur simultaneously also in the presence of multiple scattering, the resulting matrix elements reflect several lumped effects, thus hindering extraction, quantification, and interpretation of the constituent intrinsic polarimetry characteristics. Various types of inverse analysis strategies have therefore been developed to delineate individual intrinsic polarimetry characteristics from a lumped system Mueller matrix. Among these, the polar decomposition of Mueller matrix, originally proposed by Lu and Chipman, has been the most widely explored approach.[31]

The polar decomposition consists of representing $\boldsymbol{M}$ as a product of three basis matrices

$$M \Leftarrow M_\Delta . M_R . M_D. \tag{1}$$

Here the matrix $\boldsymbol{M}_\Delta$ describes the depolarizing effects of the medium, the effects of linear and circular retardance (or optical rotation) are contained in M_R, and M_D includes the effects of linear and circular diattenuation. Note that while such product decomposition was originally developed for 4×4 matrix, a similar procedure for the decomposition of the 3×3 submatrix (which involve linear polarization descriptors only, thus excludes the fourth row and fourth column of Mueller matrix involving circular polarization description) has also been developed and validated.[37] The 3×3 Mueller matrix considerably simplifies the polarimetric measurement and analysis procedure because it uses linear polarization states only in its polarization state generator (PSG) and polarization state analyzer (PSA) units. Thus the need for cumbersome calibration of the wavelength variations of PSG and PSA (which usually arise due to the wavelength response of the retarding elements for generating/analyzing circular/elliptical states) are taken care of while measuring (constructing) spectral (at multiple wavelengths) Mueller matrices from any sample. We have therefore adopted the 3×3 Mueller matrix measurements and decomposition for our study, which involve spectroscopic measurements. The process for 3×3 Mueller matrix decomposition is briefly summarized below.

2.1 *Decomposition of 3×3 Mueller Matrix*

In the 3×3 Mueller matrix decomposition also, the measured Mueller matrix M is represented as the product of three basis matrices as in Eq. (1). Here the 3×3 diattenuation matrix (M_D) is constructed using the elements M (1, 2) and M (1, 3) of the first row of the matrix M. The corresponding magnitude of linear diattenuation (d) is derived as[37]

$$d = \frac{1}{M(1,1)} \sqrt{M(1,2)^2 + M(1,3)^2}. \tag{2}$$

The inverse of the diattenuation matrix M_D is then multiplied with the recorded Mueller matrix M to remove the diattenuation effect. The remaining matrix (M') can be represented as a product of 3×3 retardance and depolarization matrices

$$M' \Leftarrow M M_D^{-1} = M_\Delta M_R. \tag{3}$$

In order to remove the contribution of depolarization, a matrix M_u is constructed from the remaining M' matrix as

$$M_u = M'(M')^T. \tag{4}$$

Using the standard form of general 3×3 retarder matrix (linear and circular retardance), it can be shown that one of the eigenvalues of the matrix M_u is unity. The other two eigenvalues for a depolarizing system would be a^2 and $a^2 \cos^2 \delta$, where δ is the linear retardance and the coefficient a is related to the linear depolarization coefficient ($\Delta = 1 - a$). Note that this generalization is based on the assumption that the linear depolarization coefficient for incident horizontal/vertical (0/90 deg) and $+45/-45$ deg states are equal ($\Delta_{0/90\,\mathrm{deg}} = \Delta_{+45/-45\,\mathrm{deg}} = \Delta$) (Refs. 27, 31, and 37). Such assumption would indeed be valid for depolarization due to multiple scattering effects (which is the primary cause of depolarization in turbid biosamples), where depolarization is isotropic in nature.[27,37] The eigenvalues of the matrix M_u can therefore be used to determine the linear depolarization coefficient Δ, and the corresponding 3×3 depolarization matrix in such case can be written as

$$M_\Delta = \begin{pmatrix} 1 & 0 & 0 \\ 0 & 1-\Delta & 0 \\ 0 & 0 & 1-\Delta \end{pmatrix}. \tag{5}$$

Finally, the 3×3 retarder matrix M_R is constructed by multiplying the inverse of M_Δ to the matrix M'. The values for linear retardance (δ) and optical rotation (ψ) can be determined from the various elements of the matrix M_R (Ref. 37)

$$\delta = \cos^{-1} \times \left(\sqrt{\{[M_R(2,2)+M_R(3,3)]^2 + [M_R(2,3)-M_R(3,2)]^2\}} - 1 \right) \tag{6}$$

$$\psi = \frac{1}{2} \tan^{-1} \left\{ \frac{[M_R(2,3) - M_R(3,2)]}{[M_R(2,2) + M_R(3,3)]} \right\}. \tag{7}$$

The above decomposition can be applied to experimentally recorded spectral 3×3 Mueller matrices to yield wavelength variation of the polarization parameters, linear depolarization coefficient [$\Delta(\lambda)$], linear diattenuation [$d(\lambda)$], linear retardance [$\delta(\lambda)$], and optical rotation [$\psi(\lambda)$].

2.2 *Estimation of the Fractal Parameters from Light Scattering Spectra*

The fractal micro-optical parameters of any scattering sample can be determined by analyzing either the angular or wavelength

variation of elastic scattering signal via appropriate light scattering models.[22–26] Note, however, that such models are usually based on single (or weak) scattering approximation, and the signature of self-similarity in the light scattering spectra are expected to be obscured due to contributions from multiply scattered light. The contribution of multiple scattering is unavoidable in the elastic scattering signal recorded from the bacterial colony samples investigated in our study (as will be apparent from nonzero values of depolarization coefficient Δ for these samples, presented subsequently). One would thus need to develop a strategy to remove/reduce the contribution of multiply scattered photons in the light scattering spectra for fractal analysis. Since multiple scattering leads to depolarization of light, the contribution of multiple scattering is expected to be minimal in the polarization-preserving component of the sample-scattered light.[21,22,27] A simplified variant of such strategy is to excite the scattering sample by linearly polarized light and record both the co-polarized ($I_{\parallel}$) and cross-polarized ($I_{\perp}$) component of scattered light. The polarization-preserving component is then extracted by subtraction of the cross-polarized component from the co-polarized component ($I^{\mathrm{pol}} = I_{\parallel} - I_{\perp}$), assuming that depolarized light contributes equally to both the polarization channels.[21,22,27] Although such strategies have previously been explored in turbid depolarizing media,[21,22] a more encompassing and generally applicable method is required for complex systems exhibiting several simultaneous polarization effects in presence of multiple scattering (the bacterial colonies that exhibit simultaneous depolarization, linear retardance, and diattenuation effects, discussed subsequently). This follows because the other nondepolarizing but polarization altering interactions (retardance and diattenuation) lead to significant alterations in both the co-polarized and cross-polarized intensity components, resulting in erroneous estimation of the polarization-preserving intensity component and its wavelength dependence. In order to tackle this problem, we have therefore explored the decomposition process described in the previous section. Note that the depolarization coefficient [$\Delta(\lambda)$], derived via the decomposition process, represents pure depolarizing transfer function (arising from multiple scattering) of the medium and is free from other polarization altering effects (retardance and diattenuation).[27] The undepolarized component of the intensity and its wavelength dependence can therefore be extracted in a more generalized way from the measured spectral 3×3 Mueller matrices and its decomposed components as

$$I^{\mathrm{pol}}(\lambda) = [1 - \Delta(\lambda)] M_{11}(\lambda), \tag{8}$$

where $M_{11}(\lambda)$ is the unnormalized first element (representing the total intensity of scattered light) of the recorded 3×3 Mueller matrix. The undepolarized component of intensity will have minimal contribution of multiply scattered photons because those will be depolarized to a larger extent. Thus extracted undepolarized part of the scattered intensity [$I^{\mathrm{pol}}(\lambda)$] may then be subjected to the fractal analysis model, to yield the fractal micro-optical parameters of the sample, as described below.

For weakly fluctuating (magnitude of refractive index fluctuation Δn is low) scattering media, the elastic scattering signal can be modeled suitably with Born approximation of light scattering.[22–25] Such an approximation has been shown to be valid for biological scatterers since the refractive index fluctuations are typically small ($\Delta n \sim 0.01$ to 0.02).[22–25,28] In the Born approximation, the expression for scattered light intensity (for any wavelength λ) at any scattering angle γ can be derived from the Fourier transformation of the refractive index spatial correlation function $C(r)$ as[22]

$$I(q) = k^4 \int C(r) \exp(iq.r) \mathrm{d}^3 r. \tag{9}$$

Here r is the correlation distance, $k = 2\pi/\lambda$ is the wave vector, and $q = 2k \sin(\gamma/2)$ is the scattering vector. Note that the parameter q can also be interpreted as the spatial frequency.

In order to describe light scattering from self-similar (fractal) biological scatterers, various types of refractive index spatial correlation functions $C(r)$ have been proposed.[22–26] Among these, the von Karman self-affine function, which is a generalized correlation function for statistically random fractal fields, has been found to be suitable.[22,26] The von Karman correlation function is given by

$$C(r) \propto \left(\frac{r}{L}\right)^{H} K_H\left(\frac{r}{L}\right). \tag{10}$$

Here, H is the Hurst exponent (a measure of the fractal nature such that it varies $0 < H < 1$ for fractals),[38–41] L is the fractal upper scale, and K_H is the modified Bessel function of the second kind of order H.

The Fourier transformation of the von Karman correlation function thus yields the analytical expression of light scattering signal as[22]

$$F(q) = I(q) \times k^{-4} \approx \frac{1}{[1 + (qL)^2]^{\alpha}}. \tag{11}$$

Here the exponent α and the Hurst exponent H are related by

$$\alpha = H + \frac{D_E}{2}. \tag{12}$$

D_E is the Euclidean dimension of the scatterers.

If the fractal upper scale is much larger than the wavelength of light ($qL \gg 1$), Eq. (11) exhibits exact inverse power law behavior

$$F(q) \approx (qL)^{-(2H + D_E)}. \tag{13}$$

Note that for the bacterial colony patterns, the fractal upper scale (L) is typically very high (typical size in mm). Thus the scattering spectra $F(q)$ exhibited the inverse power law behavior (results shown later). The undepolarized component of the light scattering spectra [$I^{\mathrm{pol}}(q)$, varying wavelength λ, fixed scattering angle γ], extracted via Eq. (8), can thus be used in Eqs. (11) and (13) to yield the exponent α. The Hurst exponent H can be determined subsequently from the value of α.

3 Experimental Methods and Materials

3.1 *Bacterial Strain and Growth Conditions*

Bacillus thuringiensis, KPWP1 was isolated from Kolkata port water.[8] Bacterial suspension of 5 μl of volume containing about 5×10^4 colony forming units was inoculated at the center of the semi-solid nutrient agar plates (5 g/l peptone, 3 g/l beef extract, 5 g/l Nacl) in absence or presence of either 1% glucose

or 3 mM sodium arsenate. Plates were incubated at 30°C and were allowed to grow for eight days. The dynamics of *Bacillus thuringiensis* colony growth was studied under three different growth conditions, in the presence of 1% glucose as additional nutrients, but under catabolic repression for flagella mediated swarming motility, in presence of 3 mM sodium arsenate as toxic material, and in their absence (normal nutrient agar environment named as control, representing favorable growth environment). Note that arsenate is always toxic to any form of life, but some bacteria have evolved with abilities to tolerate or detoxify the toxic effect of arsenate in growth environment. We have observed that the isolated *Bacillus thuringiensis* strain KPWP1 can tolerate up to 6 mM of sodium arsenate in their growth medium (data not shown). We have accordingly used a concentration of 3 mM sodium arsenate (in nutrient agar plates) to study the pattern and the dynamics of colony growth of *Bacillus thuringiensis* KPWP1 under such conditions. The images for the patterns formed during bacterial growth were acquired using Gel Documentation System (Bio-rad) and "Quantity One" software.[8]

3.2 *Experimental Methods*

A schematic of the experimental setup for the measurement of spectral 3×3 Mueller matrices is shown in Fig. 1. Briefly, the system comprises a collimated output from a Xe lamp (HPX-2000, Ocean Optics, USA) as excitation source, a PSG and a PSA unit to generate and analyze polarization states required for 3×3 sample Mueller matrix measurements, coupled to a spectrometer (USB 4000FL, Ocean Optics, USA) for spectrally resolved (wavelength $\lambda = 500$ to 750 nm, resolution ~1.8 nm) signal detection. Construction of 3×3 Mueller matrix requires nine sequential measurements performed with varying linear polarizer and analyzer states. The required three linear polarization states were generated using a rotatable linear polarizer (P, forming the PSG unit) mounted on a computer-controlled rotational mount, which was sequentially rotated to three different angles ($\theta = 0$ deg, 45 deg, and 90 deg from the horizontal). The sample-scattered light collected (at user-selected detection angle γ) and collimated using an assembly of lenses, then passes through suitably oriented analyzer ($\theta = 0$ deg, 45 deg, and 90 deg forming the PSA unit), and finally the spectra are recorded using the spectrometer. These nine spectrally resolved intensity measurements were combined to yield the spectral 3×3 sample Mueller matrices, as follows.[29,37]

The PSG (**W**) and the PSA (**A**) matrices for this configuration can be written as

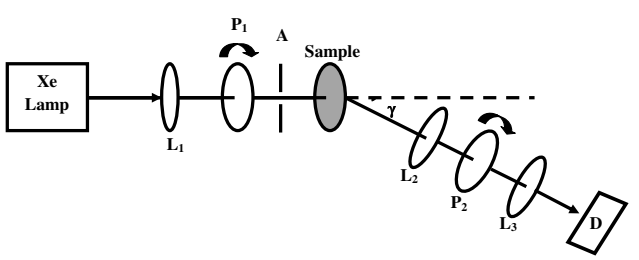

Fig. 1 A schematic of the spectral 3×3 Mueller matrix polarimeter. P_1, P_2 = linear polarizer and analyzer; L_1, L_2, L_3 = lenses; A = aperture; D = fiber optic spectrometer.

$$W = \begin{pmatrix} 1 & 1 & 1 \\ 1 & -1 & 0 \\ 0 & 0 & 1 \end{pmatrix}, \qquad A = \begin{pmatrix} 1 & 1 & 0 \\ 1 & -1 & 0 \\ 1 & 0 & 1 \end{pmatrix}. \tag{14}$$

The nine-element intensity measurement matrix $[M_i(\lambda)]$ can be related to the 3×3 sample Mueller matrix as[29,37]

$$M_i(\lambda) = A.M_S(\lambda).W. \tag{15}$$

The sample Mueller matrix, written in 9×1 vector form, can be determined as

$$M_{svec}(\lambda) = Q^{-1} M_{ivec}(\lambda), \tag{16}$$

where Q is a 9×9 matrix given as Kronecker product of A with transpose of W

$$Q = A \otimes W^T. \tag{17}$$

The spectral 3×3 Mueller matrix measurement setup was calibrated by performing measurements on standard optical elements (such as linear polarizer, quarter waveplates, etc.). The system has been completely automated and is capable of Mueller matrix measurement with reasonable accuracy (elemental error $\leq \pm 0.025$) over the entire spectral range of 500 to 750 nm. The spectral 3×3 Mueller matrices were recorded from the *Bacillus thuringiensis* colony samples in the forward-scattering geometry. Typical spot size of the collimated light incident on the sample was ~1 mm. Note that the signature of larger sized scatterers (dimension $> \lambda$) are generally more prominent in forward-scattering angles, and reverse is the case for smaller sized scatterers (whose signature are more prominent at large scattering angles). Since the dimension of the scatterers (typical dimension 1 to 3 μm) and the spatial scale of fractality of the bacterial colonies are larger than the wavelength of light, the elastic scattering spectra were recorded from the samples at smaller forward-scattering angle ($\gamma = 15$ deg).

Following the Mueller matrix spectroscopic studies, optical microscopic investigations were performed from similar regions of the *Bacillus thuringiensis* colonies (at the periphery of the growing colonies). For this purpose, a loop-full of bacterial culture of *Bacillus thuringiensis* strain KPWP1 was taken from the edge of the growing bacterial colony, stained with crystal violet solution, and observed under 100× oil immersion objective using Olympus IX51 inverted microscope. Electron microscopic studies of *Bacillus thuringiensis* KPWP1 cells from growing edge of bacterial colonies were also performed to find details of bacterial morphology and ultra-structures under different growth conditions. For this purpose, bacterial cells were taken, suspended in phosphate buffered saline, fixed in 2% paraformaldehyde, and then applied on carbon-coated copper grid. Fixed bacteria on carbon-coated copper grids were viewed under a transmission electron microscope (FEI, Model: TECHNAI-S-TWIN), with a magnification 2100×.[8]

The ultra-structural information obtained from the optical and electron microscopic studies were used to understand and corroborate some of the findings of the Mueller matrix spectroscopic studies (the derived fractal micro-optical parameter and the intrinsic polarization parameters and their dependence on the growth conditions).

4 Results and Discussion

The images for the patterns formed during bacterial growth under the three different conditions are shown in Fig. 2. In agreement with the results of our previous study,[8] here also, presence of 1% glucose in growth medium caused initially a slower but more opaque radial growth of bacterial colony as compared with that for normal nutrient agar environment (control sample). This was followed by (after four days of growth) emergence of branching pattern, as noted in Fig. 2(b). In contrast to this, presence of 3 mM arsenate in growth medium caused slowing down of overall growth of *Bacillus thuringiensis* colonies and moreover, appearance of translucent layer was observed along with branching pattern of colony growth [Fig. 2(c)].

In order to probe the structural changes taking place during the colony formations under different conditions, spectroscopic Mueller matrix measurements and inverse analysis were performed from the same samples. Figure 3 shows typical spectral 3×3 Mueller matrix recorded from the peripheral region of the growing colony with 1% glucose. In order to show the spectral variation, un-normalized Mueller matrix elements are shown in the figure. The complex nature of the Mueller matrix elements, with all nine nonzero elements (and their spectral variation), underscores the fact that the bacterial colony samples exhibit simultaneous several polarization effects including depolarization. The spectral Mueller matrices were therefore subjected to the decomposition analysis (described in Sec. 2.1) to yield the constituent basis matrices of the individual polarimetry effects. The polarization-preserving component of the scattered light and its spectral variation was extracted and were subjected to the fractal analysis following the procedure described in Sec. 2.2. The variation of the undepolarized component of the light scattering signal with wavelength λ [$F(q) = I(q) \times k^{-4}$, $q = 4\pi/\lambda \sin(\lambda/2)$, of Eq. (11), the scattering vector q has been converted to wavelength, in order to display as a function of λ] is shown in Fig. 4(a) (displayed in log-log scale). The corresponding variations of the light scattering signal for the bacteria colonies growing in normal nutrient agar environment (control) and in presence of 3 mM sodium arsenate are shown in Fig. 4(b) and 4(c), respectively. The inverse power law dependence of F is apparent from the linear decay in the log scale [$\log(F)$ versus $\log(\lambda)$] over a broad range of wavelengths, a clear manifestation of the self-similar (fractal) organization of the scattering structures present in the sample.[22,26] Note that determination of the fractal micro-optical parameter, the Hurst exponent, from the spectral slope using the fractal-

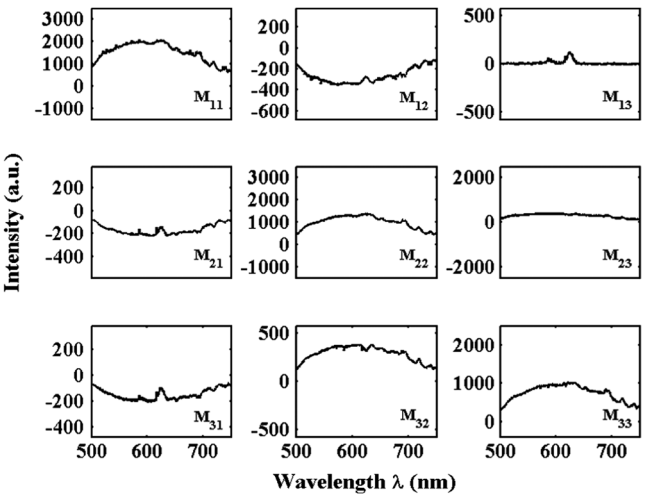

Fig. 3 Typical unnormalized spectral 3×3 Mueller matrix recorded from the peripheral region of the *Bacillus thuringiensis* colony growing in presence of 1% glucose.

Born approximation based model presented in Eqs. (11) to (13), is based on the assumption that there is no additional (other than scattering) modulation in the spectral variation arising due to other effects such as absorption. However, apparently the spectra recorded from the bacteria colony growing in presence of 1% glucose [Fig. 4(a)] and in presence of 3 mM sodium arsenate [Fig. 4(c)] shows a spectral dip beyond the wavelength $\lambda = 640$ nm (0.64 μm), possibly due to the signature of some absorption effects. Thus, in order to avoid any artifact in the determination of Hurst exponent, the linear region of $\log(F)$ versus $\log(\lambda)$ ($\lambda = 560$ to 640 nm, corresponding log λ: -0.58 to -0.45, λ represented in μm in the figures) was chosen. For the bacteria colony growing in normal nutrient agar environment [control, Fig. 4(b)], the absorption dip was observed to shift toward shorter wavelength ($\lambda \sim 580$ μm), shifting the linear region of $\log(F)$ versus $\log(\lambda)$ to between $\lambda = 530$ and 580 nm (corresponding log λ: -0.63 to -0.54, when λ is represented in μm), and this was accordingly used in the fractal analysis.

The values for the exponent α and the Hurst exponent H [using Eq. (13)] for the bacteria colony growing in presence of 1% glucose was estimated to be 1.87 and 0.37, respectively. The signature of self-similarity obtained from the light scattering spectra actually originates from the spatial fluctuations in the

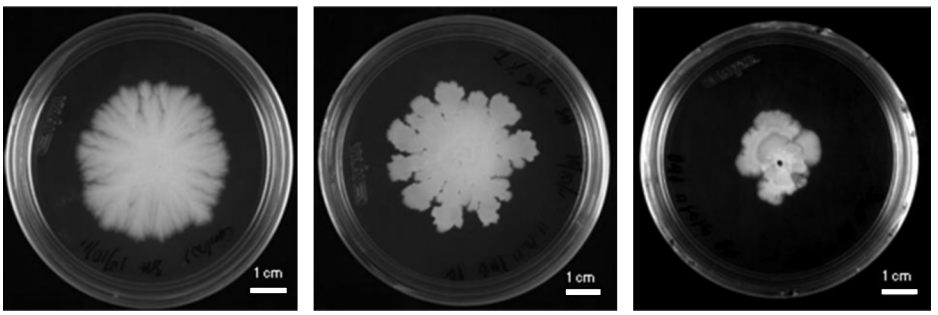

(a) Control (b) 1% Glucose (c) 3mM arsenate

Fig. 2 The images for the bacterial growth patterns of *Bacillus thuringiensis* KPWP1 formed under the three different conditions: (a) normal nutrient agar environment (control, representing favorable growth environment); (b) nutrient agar supplemented with 1% glucose as additional nutrient; and (c) nutrient agar supplemented with 3 mM sodium arsenate as toxic material. The scale bars shown at bottom corner represent 1 cm length.

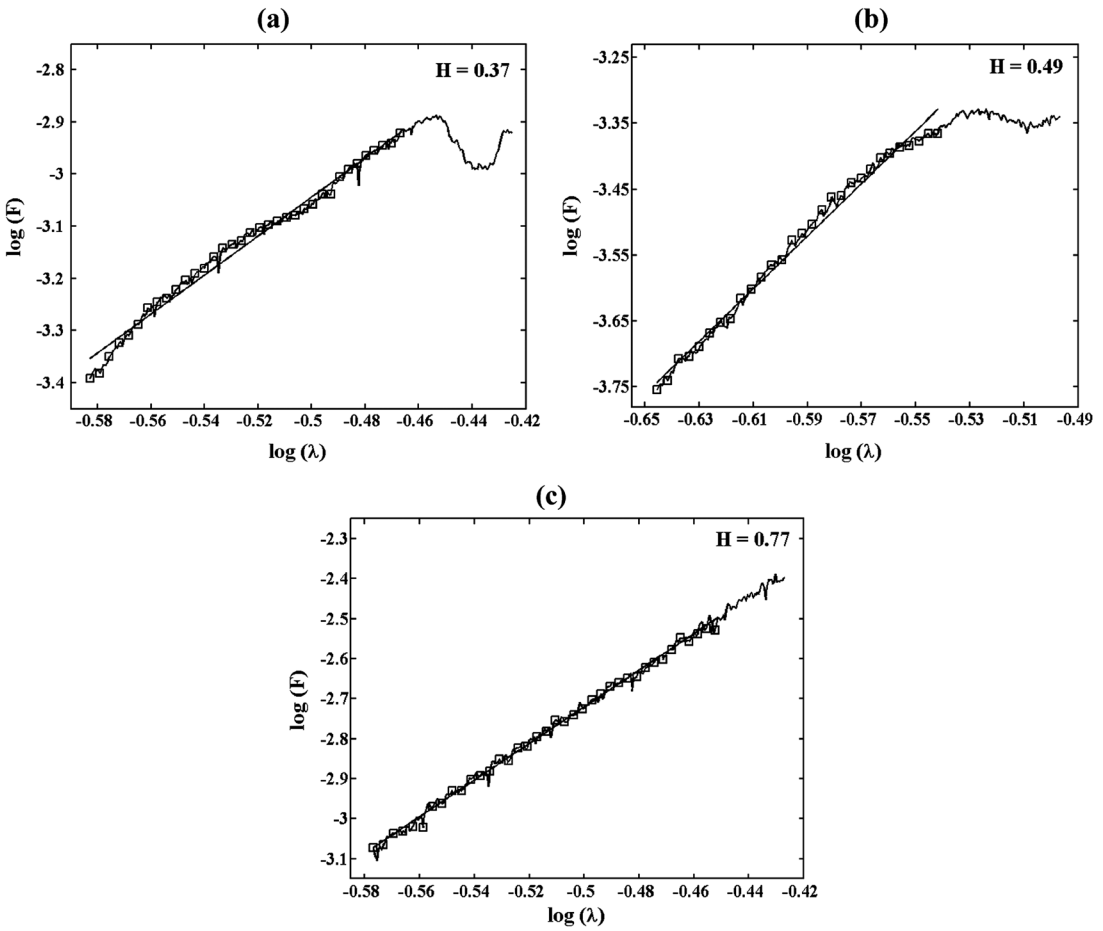

Fig. 4 The variation of the undepolarized component of the light scattering signal with wavelength (λ) (displayed in log-log scale, λ is shown here in μm) recorded from *Bacillus thuringiensis* colony growing: (a) in presence of 1% glucose; (b) in normal nutrient agar environment (control); and (c) in presence of 3 mM sodium arsenate. The linear region of $\log(F)$ versus $\log(\lambda)$ was chosen for the fractal analysis [linear fitting using Eq. (13) to estimate the spectral slope and resulting Hurst exponent]. For the bacteria colony growing in presence of 1% glucose: (a) and in presence of 3 mM sodium arsenate; (c) this range was $\lambda = 560$ to 640 nm [corresponding log λ: −0.58 to −0.45 (λ in μm)]. For the bacteria colony growing in normal nutrient agar environment (b); the range was $\lambda = 530$ to 580 nm (log λ: −0.63 to −0.54). The linear fits (in log-log scale) are displayed by solid line in each figure and the corresponding estimates for Hurst exponent H are also noted in the figures.

local refractive index structures (scattering centers), with the former containing information about the latter in the Fourier domain [as apparent from Eq. (9)].[22,26] The estimated value for H can therefore be regarded as the representative statistical self-similarity of the spatial refractive index fluctuations.[26] The limiting values of H, unity and zero, for such statistical fractals (fluctuations) correspond to a smooth Euclidean random field (marginal fractal) and a space-filling field (extreme fractal), respectively.[40] Moreover, in terms of the statistical nature of such fluctuations, $H = 0.5$, $H > 0.5$, and $H < 0.5$ correspond to uncorrelated random (Brownian) fluctuations, long-range correlations, or persistent behavior and anti-correlated or anti-persistent behavior.[40] A value of $H = 0.37$ thus represents a trend toward extreme fractality and anti-correlated behavior in the index fluctuations.

The corresponding results of fractal analysis of the light scattering signal for the bacteria colonies growing in normal nutrient agar environment (control) and in presence of 3 mM sodium arsenate are shown in Fig. 4(b) and 4(c), respectively. Significant differences in the fractality descriptor, Hurst exponent (H) values are observed for bacteria colonies growing under the three different environments, indicating a strong dependence of the nature of the colony pattern on the growth environment. As evident from the figures, the bacterial colony growing in the presence of 1% glucose exhibits the strongest fractality (lowest value of H), whereas the colony growing in presence of 3 mM sodium arsenate shows the weakest fractality (a trend toward subfractal behavior). A value of H close to 0.5 (=0.49) for colony growing in normal nutrient agar environment signifies randomness of the index fluctuations (scattering structures).[40] This possibly originates from the fact that in such favorable growth environment, the colony pattern evolves randomly in all directions as bacteria grow independent of each other (in an uncorrelated manner) in hunt for food. The strong fractality of the colony growth pattern in presence of 1% glucose, on the other hand, may be resulting from the closely associated cooperative behavior of the bacteria in the presence of the additional nutrient. A lower value of H (<0.5, =0.37), in this case, accordingly indicates increasing roughness of the medium and formation of some finer organized structures (deviation from a random behavior of fluctuations to anti-correlated or anti-persistent behavior).[40] In contrast, in presence of arsenate as toxic material, the apparent hindering (because of the lack of the availability of food) of the growth of the overall colony results in much smaller colony formation. An increased value of H (>0.5, =0.77) here is characteristic of relatively smoother or

coarser scattering structure having a weaker degree of fractality. Measurements and analysis were performed from five different spots in the peripheral regions of each of the growing colonies. The results were consistent; the value for H being the lowest ($H < 0.5$) for colony growing in presence of glucose, highest for the colony growing in presence of arsenate ($H > 0.5$), and intermediate for colony growing in normal nutrient agar environment ($H \sim 0.5$).

In order to probe further the changes in the microscopic organization and structures during the colony formations under the three different conditions, the intrinsic medium polarization parameters, namely, the linear diattenuation [$d(\lambda)$], linear retardance [$\delta(\lambda)$], and linear depolarization [$\Delta(\lambda)$] coefficients, were extracted from the recorded spectral 3×3 Mueller matrices, following the procedure described in Sec. 2.1. In Fig. 5(a) and 5(b), we show the wavelength variation ($\lambda = 500$ to 750 nm) of the δ and d parameters, respectively, for the colonies growing in three different conditions. Significant values for the linear retardance δ are observed for the bacterial colony samples. The values for δ are observed to be considerably higher for bacterial colony growing in presence of 1% glucose as compared to that for normal nutrient agar environment (control) and that growing in presence of 3 mM sodium arsenate. In fact, the magnitude of linear retardance is the weakest for colony growing in the agar with no additional nutrient such as glucose or toxin such as arsenate. In addition to linear retardance, the decomposition procedure also yields appreciable values for linear diattenuation, as apparent from Fig. 5(b). A similar trend is also observed for diattenuation, with the magnitude for d being considerably higher for colonies growing in presence of 1% glucose as compared to the other two cases. Note that at macroscopic level, δ and d have a common origin, both arise from differences in refractive indices (real and imaginary parts, respectively) for different polarization states. Scattering from anisotropic (oriented) structures leads to linear retardance and diattenuation effects;[27,34] accordingly these contain useful information on anisotropic organization of scattering microstructures. The significantly enhanced value for δ and d in presence of 1% glucose is thus indicative of the presence of anisotropically organized scattering structures (organized rod-shaped bacteria) in the peripheral region of the growing colony. As predicted by the fractal analysis, the formation of such anisotropic structure is possibly a manifestation of the associated cooperative behavior of the individual bacterium in the colony. On the other hand, for the growing colony in normal nutrient agar environment, the isotropic (random) growth of bacteria over the entire colony and, accordingly, the absence of formation of anisotropic organized structures manifest as a low value of δ and d parameters. Even though the presence of arsenate as toxic material prevents natural growth and evolution of the overall colony, moderate values of δ possibly arises due to formation of smoother structures at the peripheral region due to the anisotropic nature of the growth.

Figure 5(c) shows the remaining polarimetry parameter, the linear depolarization coefficient $\Delta(\lambda)$ for the same colonies growing under the three different environments. Presence of significant depolarization for all of these colonies (specifically for

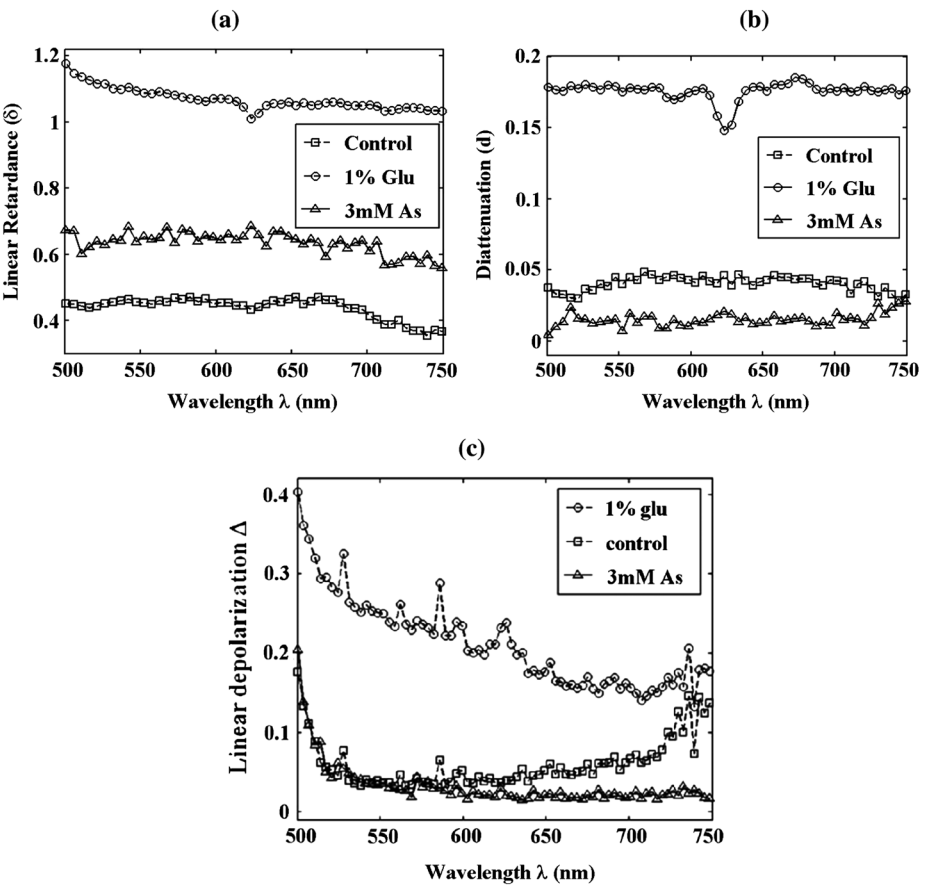

Fig. 5 The wavelength variation ($\lambda = 500$ to 750 nm) of the decomposition derived: (a) linear retardance δ; (b) linear diattenuation d; and (c) linear depolarization Δ parameters, for the *Bacillus thuringiensis* colonies growing in normal nutrient agar (open square), in the presence of 1% glucose (open circle), and in presence of 3 mM sodium arsenate (open triangle).

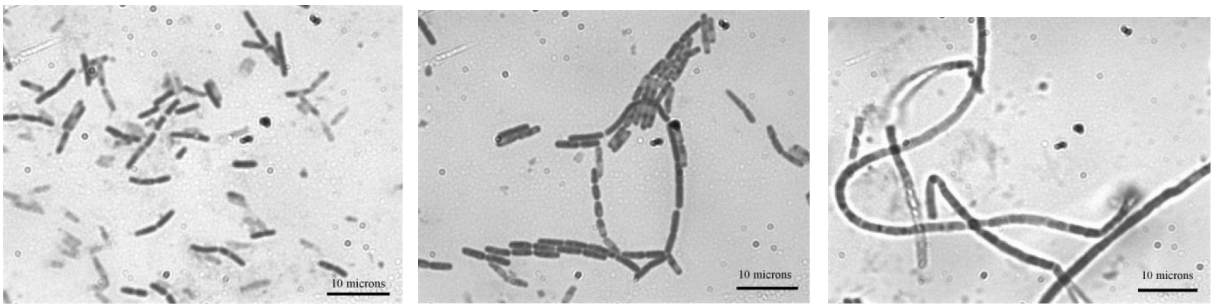

(a) (b) (c)

Fig. 6 The optical microscopic images recorded from the stained (with crystal violet solution) *Bacillus thuringiensis* colonies growing (a) in normal nutrient agar environment (control); (b) in presence of 1% glucose; and (c) in presence of 3 mM sodium arsenate. The scale bars shown at bottom corner represent 10 μm length.

colony growing in presence of 1% glucose) rationalizes the use of the decomposition analysis for the purpose of either extracting the intrinsic polarization parameters or for the fractal analysis presented before. Note that the depolarization effect in the bacteria colony samples primarily originate from multiple scattering effects within the sample (due to the presence of turbidity).[27,28] The observed significantly enhanced depolarization in the bacteria colony growing in presence of glucose is consistent with the observed lower value of Hurst exponent ($H = 0.37$), derived via the fractal analysis. As previously noted, decreasing Hurst exponent implies increasing roughness of the medium or formation of finer scattering structures, which causes stronger multiple scattering within the sample, leading to much stronger depolarization.[27] In contrast, in presence of 3 mM arsenate as toxic material, formation of smoother or coarser scattering structures (as inferred from considerably increased value of $H > 0.5$, $=0.77$) leads to weakening of multiple scattering effects and subsequent reduction of net depolarization Δ. In accordance with this interpretation, bacterial colony growing in normal nutrient agar exhibited intermediate depolarization values.

In order to comprehend further the polarimetric light scattering findings presented above, in Fig. 6(a), 6(b), and 6(c), we present the microscopic images recorded from the stained (with crystal violet solution) *Bacillus thuringiensis* colonies growing under the three different environments. Several observations are at place: (1) In conformity with the predictions of the fractal and the inverse polarimetry analysis, the *Bacillus thuringiensis* cells growing in normal nutrient agar environment shows existence of randomly distributed small rod-shaped bacteria [Fig. 6(a)]. This is a common characteristic of any bacteria of *bacilli* genera, growing independent of each other in search for food in the favorable environment. The lack of the organization of the scattering structures (rod-shaped bacteria) leads to considerably lower value of linear retardance δ and diattenuation d coefficients and accordingly nonzero values for depolarization Δ coefficient. Moreover, the randomness of index fluctuations is also reflected in the Hurst exponent, H, value which is close to 0.5 ($H = 0.49$). (2) In presence of 1% glucose, formation of closely associated long chains of bacteria in the form of rafts, as signature of bacterial cooperative behaviour, is evident [Fig. 6(b)]. While formation of such organized anisotropic domains of scattering structures leads to the enhancement of δ and d parameters, a much denser distribution of the scatterers results in subsequent increase of the depolarization Δ parameter. (3) In presence of arsenite, the *Bacillus thuringiensis* cells form elongated filamentous structures to survive and grow in the toxic environment. This leads to apparent loss of fractality and a trend toward smoother index fluctuations ($H > 0.5$). The long filamentous structures may thus lead to lower value of depolarization Δ coefficient and some residual value for linear retardance δ parameter, despite having much weaker fractality. The electron microscopic images also confirmed presence of bacterial cells with significantly larger dimension, when grown in presence of 3 mM sodium arsenate (results not shown here).

The combined fractal micro-optical properties and the intrinsic polarization parameters thus yielded complementary, useful, and otherwise hidden information on the microstructural organization, cellular association, and patterns of the bacterial colony growing under different environments. Derivation, quantification, and interpretation of the morphological information is exclusively enabled by spectral light scattering polarimetric measurements and its subsequent analysis via combined polar decomposition of Mueller matrix and Born approximation-based fractal-light scattering approach.

5 Conclusions

We have explored the use of quantitative spectral light scattering polarimetry to probe the morphological and structural changes of growing *Bacillus thuringiensis* bacteria colonies under different environments. The method is based on measurement of spectral 3×3 Mueller matrices and its subsequent analysis, via polar decomposition to extract the intrinsic polarization parameters, and Born approximation-based inverse analysis of the polarization-preserving component of the light scattering spectra to yield the fractal Hurst parameter. Interesting differences were noted in the Hurst exponent, H, and the intrinsic polarization parameters (linear diattenuation d, linear retardance δ, and linear depolarization Δ coefficients) of the bacterial colonies growing under different conditions (in normal nutrient agar environment and in absence or presence of 1% glucose or 3 mM sodium arsenate). The bacterial colony growing in presence of glucose as additional nutrient exhibited the strongest fractality (lowest value of H), whereas the colony growing in presence of sodium arsenate as toxic material showed the weakest fractality. Moreover, the values for δ and d parameters were also found to be considerably higher for the colony growing in presence of glucose, indicating more structured and organized growth pattern. The findings of the polarimetry and light scattering spectroscopic measurements/analysis were corroborated further with optical microscopic studies conducted on the same samples. The intrinsic polarization parameters and fractal micro-optical

properties, derived via the spectral light scattering polarimetric approach, thus hold promise as useful biological metrics for quantification of cellular association and patterns in growing bacterial colony. In general, such novel polarimetry method may facilitate a nondestructive way for *in situ* monitoring, detection, and identification of a bacterial species in a given space and under a given set of conditions, an important example of which has been illustrated in this study.

Acknowledgments

This work was supported by Indian Institute of Science Education and Research, Kolkata, an autonomous teaching and research institute funded by the Ministry of Human Resource Development, Government of India. The authors wish to thank transmission electron microscope facility of Saha Institute of Nuclear Physics, Kolkata, India. P.B. thanks Council of Scientific and Industrial Research, Government of India for research fellowship.

References

1. T. P. Curtis, W. T. Sloan, and J. W. Scannel, "Estimating prokaryotic diversity and its limits," *Proc. Natl. Acad. Sci.* **99**(16), 10494–10499 (2002).
2. S. Freilich et al., "Competitive and cooperative metabolic interactions in bacterial communities," *Nat. Commun.* **2**, 589 (2011).
3. S. Swift et al., "Quorum sensing as a population density dependent determinant of bacterial physiology," *Adv. Microb. Physiol.* **45**, 199–270 (2001).
4. E. B. Jacob et al., "Generic modeling of cooperative growth patterns in bacterial colonies," *Nature* **368**(6466), 46–49 (1994).
5. E. B. Jacob et al., "Bacterial cooperative organization under antibiotic stress," *Physica A* **282**(1–2), 247–282 (2000).
6. J. A. Bonachela et al., "Universality in bacterial colonies," *J. Statist. Phys.* **144**(2), 303–315 (2011).
7. J. Y. Wakano et al., "Self-organized pattern formation of a bacteria colony modeled by a reaction diffusion system and nucleation theory," *Phys. Rev. Lett.* **90**(25), 258102 (2003).
8. M. K. Roy et al., "Glucose induced fractal colony pattern of Bacillus thuringiensis," *J. Theor. Bio.* **265**(3), 389–395 (2010).
9. E. B. Jacob and P. Garik, "The formation of patterns in non-equilibrium growth," *Nature* **343**(6258), 523–530 (1990).
10. E. B. Jacob, "Social behavior of bacteria: from physics to complex organization," *Eur. Phys. J. B* **65**(3), 315–322 (2008).
11. A. Chattopadhyay, N. B. Bhatnagar, and R. Bhatnagar, "Bacterial insecticidal toxins," *Crit. Rev. Microbiol.* **30**(1), 33–54 (2004).
12. A. S. Griffin, S. A. West, and A. Buckling, "Cooperation and competition in pathogenic bacteria," *Nature* **430**(7003), 1024–1027 (2004).
13. M. E. Hibbing et al., "Bacterial competition: surviving and thriving in the microbial jungle," *Nat. Rev. Microbiol.* **8**(1), 15–25 (2010).
14. B. Rajwa et al., "Phenotypic analysis of bacterial colonies using laser light scatter and pattern-recognition techniques," *Proc. SPIE* **6864**, 68640S (2008).
15. A. S. Ul'yanov, "Analysis of fractal dimensions in the express diagnostics of bacterial colonies," *Opt. Spectrosc.* **107**(6), 866–872 (2009).
16. P. P. Banada et al., "Label-free detection of multiple bacterial pathogens using light-scattering sensor," *Biosens. Bioelectron.* **24**(6), 1685–1692 (2009).
17. E. B. N. Bai et al., "Modeling light propagation through bacterial colonies and its correlation with forward scattering patterns," *J. Biomed. Opt.* **15**(4), 045001 (2010).
18. V. A. Bloomfield, "Quasi-elastic light scattering applications in biochemistry and biology," *Annu. Rev. Biophys. Bioeng.* **10**(1), 421–450 (1981).
19. N. N. Boustany, S. A. Boppart, and V. Backman, "Microscopic imaging and spectroscopy with scattered light," *Annu. Rev. Biomed. Eng.* **12**(1), 285314 (2010).
20. V. V. Tuchin, *Tissue Optics: Light Scattering Methods and Instruments for Medical Diagnosis*, pp. 1–825, SPIE Press, Bellingham (2007).
21. S. Gurjar et al., "Imaging human epithelial properties with polarized light-scattering spectroscopy," *Nat. Med.* **7**(11), 1245–1248 (2001).
22. M. Hunter et al., "Tissue self-affinity and polarized light scattering in the born approximation: a new model for precancer detection," *Phys. Rev. Lett.* **97**(13), 138102 (2006).
23. I. R. Capoglu et al., "Accuracy of the Born approximation in calculating the scattering coefficient of biological continuous random media," *Opt. Lett.* **34**(17), 2679–2681 (2009).
24. C. J. R. Sheppard, "Fractal model of light scattering in biological tissue and cells," *Opt. Lett.* **32**(2), 142–144 (2007).
25. M. Xu and R. R. Alfano, "Fractal mechanisms of light scattering in biological tissue and cells," *Opt. Lett.* **30**(22), 3051–3053 (2005).
26. J. M. Schmitt and G. Kumar, "Turbulent nature of refractive-index variations in biological tissue," *Opt. Lett.* **21**(16), 1310–1312 (1996).
27. N. Ghosh and A. I. Vitkin, "Tissue polarimetry: concepts, challenges, applications, and outlook," *J. Biomed. Opt.* **16**(11), 110801–110829 (2011).
28. V. V. Tuchin, L. Wang, and D. À. Zimnyakov, *Optical Polarization in Biomedical Applications*, Springer-Verlag, Berlin, Heidelberg, NY (2006).
29. R. A. Chipman, "Polarimetry," in *Handbook of Optics*, 2nd ed., M. Bass, Ed., Vol. 2, pp. 22.1–22.37, McGraw-Hill, New York (1994).
30. W. S. Bickel and W. M. Bailey, "Stokes vectors, Mueller matrices, and polarized scattered light," *Am. J. Phys.* **53**(5), 468–478 (1985).
31. S. Y. Lu and R. A. Chipman, "Interpretation of Mueller matrices based on polar decomposition," *J. Opt. Soc. Am. A* **13**(5), 1106–1113 (1996).
32. R. Ossikovski et al., "Depolarizing Mueller matrices: how to decompose them?" *Phys. Stat. Sol. (a)* **205**(4), 720–727 (2008).
33. R. Ossikovski, A. D. Martino, and S. Guyot, "Forward and reverse product decomposition of depolarizing Mueller matrices," *Opt. Lett.* **32**(6), 689–691 (2007).
34. N. Ghosh, M. Wood, and A. Vitkin, "Polarized light assessment of complex turbid media such as biological tissues using Mueller matrix decomposition," in *Handbook of Photonics for Biomedical Science* V. V. Tuchin, Ed., pp. 253–282, Taylor and Francis Publishing, NewYork (2010).
35. N. Ghosh, M. F. G. Wood, and I. A. Vitkin, "Mueller matrix decomposition for extraction of individual polarization parameters from complex turbid media exhibiting multiple scattering, optical activity, and linear birefringence," *J. Biomed. Opt.* **13**(04), 044036 (2008).
36. N. Ghosh et al., "Mueller matrix decomposition for polarized light assessment of biological tissues," *J. Biophoton.* **2**(3), 145–156 (2009).
37. M. K. Swami et al., "Polar decomposition of 3×3 Mueller matrix: a tool for quantitative tissue polarimetry," *Opt. Express* **14**(20), 9324–9337 (2006).
38. H. Hurst, "Long-term storage capacity of reservoirs," *Trans. Am. Soc. Civ. Eng.* **116**, 770–808 (1951).
39. B. Mandelbrot, *The Fractal Geometry of Nature*, pp. 1–468, W. H. Freeman and Co., San Francisco (1982).
40. W. Kantelhardt et al., "Multi-fractal detrended fluctuation analysis of nonstationary time series," *Physica A* **316**(1–4), 87–114 (2002).
41. S. Ghosh et al., "Differing self-similarity in light scattering spectra: a potential tool for pre-cancer detection," *Opt. Express* **19**(20), 19717–19730 (2011).